Simulation Studies of a Trench MOS Device Structure with Small Figures of Merit

Junhong Li

State Key Laboratory of Electronic Thin Films and Integrated Devices, University of Electronic Science and Technology of China

Abstract. We proposed a vertical high permittivity trench power MOS (HKTMOS) device with alternating N&P drift region and high permittivity (HK) trench sandwiched in between. The unique structure guarantees uniform potential distribution for wide voltage range at block state owing to both HK potential modulation effect and superjunction (SJ) charge balance. The specific on-resistance (Rons) of HKTMOS is in orders of magnitude lower than the SJ counterparts at the on state because of the strong accumulation effect brought by HK trench. Although the gate charge also significantly rises because of the accumulation, the figures of merit (FOM) of HKTMOS still reduces considerably than the SJ under same BV. An expression for FOM is derived demonstrating that the FOM of HKTMOS is proportional to the square of HK trench depth, which agrees on with simulation results well. The simulation results indicate that within the BV range of 500~2000V, the Rons and FOM of HKTMOS are in 1~2 orders of magnitude lower and 17.4%~44.1% of SJ, respectively under the same BV condition. Furthermore, HKTMOS also demonstrates better charge imbalance tolerance than SJ.

1 Introduction

The performance of silicon power devices are essential for the energy conversion system. The introduction of high permittivity (HK) material into power MOS device allows better potential distribution in silicon and therefore improves device breakdown voltage (BV) [1]. The effect is called the HK potential modulation (PM) effect [1], which had been demonstrated both theoretically [2] and experimentally[3]. On other hand, because HK material exhibits large permittivity, it is potential to be used to activate the carrier accumulation (CA) effect in silicon to significantly reduce the device on-resistance (Ron). In this letter, we propose a novel HK trench MOS (HKTMOS), which utilizes both PM and CA effects from HK, resulting in specific-Ron(R_{ons}) decrease in orders of magnitude compared with conventional superjunction device (SJ). Although such R_{ons} decrease is at the cost of larger switch loss due to the extra accumulation charge on the gate, the relationship between R_{ons} and gate charge is linear, and the total figures of merit (FOM) of HKTMOS still experiences a significant improvement than the SJ. Furthermore, HKTMOS also indicated strong doping-imbalance tolerance in N and P drift region.

2 Device structure and mechanism

The cross section view of HKTMOS is showed in Figure 1a. Similar with SJ, HKTMOS also features alternating N and P drift region pillar, whereas a layer of HK material is sandwiched in between. Together with the buried oxide in the N+ drain region, the P drift region is completely isolated from the N drift region and the drain, but directly contacts with the gate.

At the device blocking state, with the same mechanism as [4], although there is HK isolation between N and P drift region, their electric field still depleted with each other because of the large permittivity of HK, so that the charge balance effect still exists. Moreover, the total permittivity of drift region is also boosted with the introduction of HK trench, according to [1], the slope of electrical field in drift region is given by (1),

$$\frac{\partial^2 \varphi}{\partial^2 x} = -\frac{\partial E}{\partial x} = -\frac{qN_d}{\varepsilon_{total}}, \quad (1)$$

Where N_d and ε_{total} are the doping concentration and total permittivity of the drift region, respectively. With large ε_{total}, the slope of the electric field is small, giving better potential distribution and higher BV on the basis on charge balance. The effect is attributing to the HK PM effect. As showed in Figure 1b, the potential distribution of HKTMOS is almost ideal at the blocking state. Besides, better doping imbalance tolerance between N and P pillar can be also realized with effect of HK, which will be verified later. Above all, at the device blocking state, both effect of HK PM and charge balance co-exists to guarantee the high BV not only for the short drift region, but also for long drift region devices.

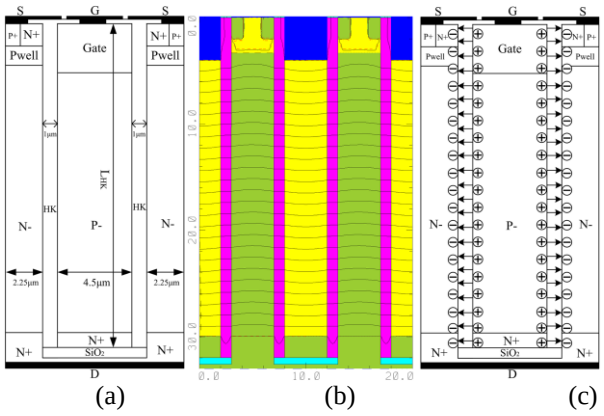

Fig 1. (a) HKTMOS cross section view with N- and P- doping of $10^{-15}cm^{-3}$. (b) Potential distribution of HKTMOS at block state. (c) Illustration of the accumulation effect.

Although the reduction of device R_{ons} by mean of CA effect has been reported in [5], the CA is generated by SiO_2 layer, with the low permittivity of SiO_2, its effect is limited. Moreover, small ε of the SiO_2 also brings negative effect for BV according to (1). On contrast, HK material is capable of overcoming the above problems. When the device in Figure 1a is in on state, the gate voltage is high, the P pillar share the same high potential with gate as their directly contact. Whereas both drain and source voltage is much lower than the gate at the on state, consequently, CA effect happens at the interface of silicon and HK trench as showed in Figure 1c. The large permittivity of HK amplified the CA effect and forms a high carrier density path between drain and source, the device R_{ons} is thereby significantly reduced.

CA effect allows significant R_{ons} reduction with no additional drift region doping. However, large trench capacitance is necessary to accumulate enough charge at the device on-state to reduce the R_{ons}. And the trench capacitor will be discharged at off-state to guarantee high BV, such charge-discharge cycle with large capacitance results in high switch loss. Rarely had any literatures qualitatively investigated such effect and its impact to FOM. For the HKTMOS device, as a low resistance path exists between drain and source generated by HK CA effect, the device R_{ons} is major determined by the accumulation resistance (R_A). According to [6], $R_A \propto 1/C_g$, where C_g is the unit area trench capacitance, we can derive that R_{ons} of HKTMOS is given by

$$R_{ons} = \frac{K_{HKT} L_{HK}}{V_g C_g W} \tag{2}$$

Where the K_{HKT}, L_{HK}, V_g, and W are the HKTMOS constant, depth of HK trench, gate voltage and width of the device, respectively. Although the N+ source junction and the drain not contributing to the total resistance are covered in the L_{HK} in (2), both of their depth are overwhelming smaller than the drift region length and thereby negligible. We see that the R_{ons} is proportional to L_{HK} for HKTMOS from (2).

On the other hand, the gate charges are contributed by both HK trenches and SiO_2 buries. The contribution from SiO_2 buries is also overwhelming smaller than the HK trenches, for both permittivity and area. Therefore, it is neglected and gate charge is given by

$$Q_g = W L_{HK} V_g C_g \tag{3}$$

According to (2) and (3), we see that the R_{ons} is inverse proportional to the gate charge for a given device dimension. The definition[6] for FOM is $FOM = R_{ons} * Q_g$, which gives

$$FOM_{HKT} = K_{HKT} L_{HK}^{\ 2} \tag{4}$$

An interesting result is observable from (4) that FOM of the HKTMOS is irrespective of the unit area trench capacitance and device width. It is only proportional to the square of the HK trench depth with ratio of HKTMOS constant K_{HKT}. According to analysis and simulation results, the analytical value of K_{HKT} is $7.812\times10^{-4}\Omega*nC/\mu m^2$.

3 Simulation verification and discussion

We use TMA-MEDICI to make 2D simulation and verify above analysis. Figure 2 shows the BV dependence for R_{ons} and switch delay for both HKTMOS with different HK permittivity ε_{HK} (a) and SJ device (b).

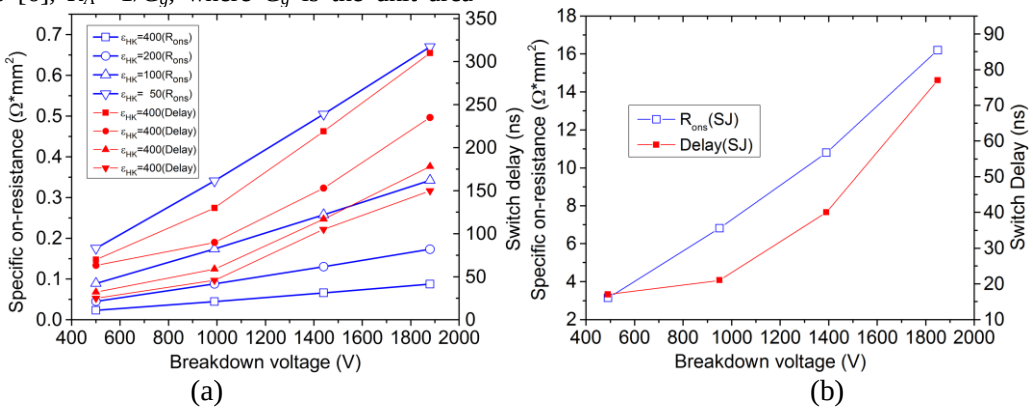

Fig 2. Under the 15 V gate voltage, the R_{ons} vs. BV and switch delay (sum of the transient rise and fall time for the drain voltage) vs. BV with a drain resistance of 4×10^6 Ω for HKTMOS (a) and 4×10^7 Ω for SJ (b) under the dimension of 20 μm×1 μm for both devices. The R_{ons} and the switching delay are simulated under a drain voltage of 0.1 V and 100 V, respectively.

As revealed in Figure 2b, the R_{ons} of the SJ rises rapidly with increase of BV at the exponential of 1.33[4]. On contrast, under the effect of strong CA effect brought by HK, the R_{ons} of HKTMOS is in the orders of magnitude lower than the SJ as showed in Figure 2a. Higher ε_{HK} always brings smaller R_{ons}, owing to the reason that higher permittivity always provides larger trench capacitance, thereby stronger CA effect and smaller R_{ons}. Moreover, expression (2) suggests that the R_{ons} of HKTMOS is proportional of the drift region length. Because the BV is also proportional to the drift region length, the R_{ons} of HKTMOS rises linearly with the increase of BV as Figure 2a reveals, which agrees on with (2).

Although the CA effect of HK reduces R_{ons} in orders of magnitude, the large trench capacitance also slow down the switching speed. As showed in Figure 2, the switch delay of the HKTMOS is much larger than the SJ device, in the orders of magnitude as well. Higher ε_{HK} value always causes worse switch delay. To investigate the comprehensive performance of the HKTMOS, the device FOMs are simulated and calculated as shown in Figure 3a. R_{ons} is simulated under the condition of a 15 V gate voltage and 0.1 V drain voltage. Q_g is simulated schematically as shown in Figure 3a, where a 15 V square wave voltage is applied on the gate. Q_g is determined by the current integral at the time interval when the drain drops from 100 V to the voltage of the fully on-state. As Figure 3a shows, both R_{ons} and Q_g increase linearly with the rise of L_{HK}, which is consistent with (3) and (5). (3) and (5) also indicated that R_{ons} and Q_g are proportional and inversely proportional to ε_{HK}, respectively. The relation is also verified by simulation, as Figure 3a shows; a larger ε_{HK} always provides a smaller R_{ons} but a larger Q_g and vice versa.

Figure 3b shows the FOM and BV vs. L_{HK} for both HKTMOS and SJ, where the FOM of HKTMOS with changing ε_{HK} are plotted in different line styles. As mentioned above, R_{ons} and Q_g are inversely proportional and proportional to L_{HK}, respectively, which cancel each other out when the multiplication for FOM occurs. It can be observed that all of the lines almost overlap with each other for different ε_{HK} when L_{HK} ranges from 30 μm to 120 μm (Figure 3b) according to simulation, which agrees with (6) very well. The proportional coefficient between the FOM and L_{HK} square may be different depending on the cell geometry; however, for a device with a given cell geometry, the FOM is only determined by L_{HK} regardless of the HK permittivity and trench thickness.

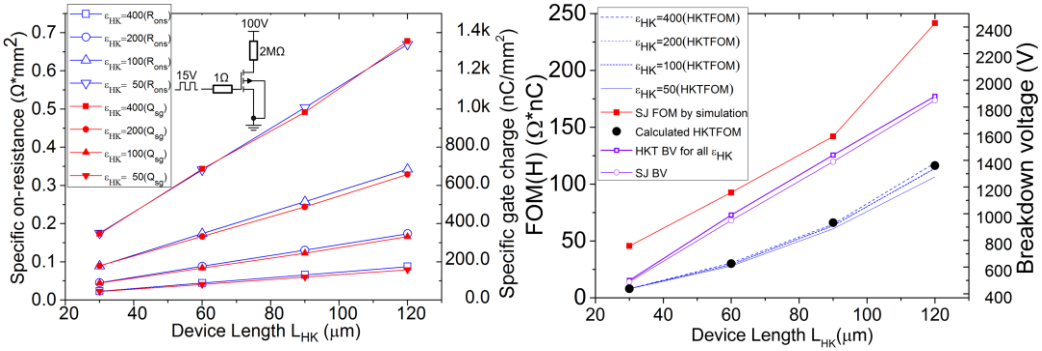

Fig 3. The R_{ons} (simulated under 15 V gate voltage and 0.1 V drain voltage) and Q_g (simulated by the integral of the gate current as the schematics show in the figure) vs. L_{HK} for HKTMOS (a) The FOM(H) vs. L_{HK} for HKTMOS by both simulation and calculation, together with the FOM(H) of SJ and BV by simulation (b).

For HKTMOS with the size displayed in Figure 2a, the analytical value of the proportional coefficient is derived as 7.812×10^{-3} Ω*nC/μm^2. Utilizing such a coefficient, we are able to calculate the FOM using (6), which is shown by the round dots in Figure 3b. It is clear that the calculation results agree well with the simulation results. Figure 3b also reveals that for the HKTMOS with smaller ε_{HK} (ε_{HK}=50), the FOM by simulation is slightly smaller than the calculated value, especially at larger L_{HK}. This is because Q_g is determined by the sum of Q_{HK} and Q_{DC}, then, Q_g will drop linearly with the linear decrease of ε_{HK} as long as Q_{HK} is still larger than Q_{DC} according to (4). However, as R_A parallels with R_{drift}, with smaller ε_{HK}, R_A in (2) is less dominant, and the contribution to R_{ons} from the drift region R_{drift} becomes more significant although R_A is still much lower than R_{drift}. Consequently, the total R_{ons} will rise sub-linearly with the decrease of the small ε_{HK} due to the contribution from the drift region bypass, which has been neglected in previous analysis. Moreover, according to (6), the FOM of HKTMOS is proportional to the square of L_{HK}; the square amplifies the model inaccuracy if L_{HK} is large, which causes a larger FOM difference between the calculated and simulated values under the condition of a large L_{HK} and a small ε_{HK} as shown in Figure 3b.

Figure 3b also shows the relationship between BV and L_{HK} for both HKTMOS and SJ. The BVs of HKTMOS with different ε_{HK} completely overlapped with each other so that only one curve is shown for HKTMOS. As the BV of SJ relies on CB only, while HKTMOS takes both effects of PM and CB to achieve high BV, the BV of HKTMOS will be slightly better than that of SJ, as shown in Figure 3b. Last but not least, HKTMOS always demonstrates significant FOM improvement over that of SJ under all L_{HK} in the figure; the FOM of HKTMOS is 48% of that of SJ at the L_{HK} of 120 μm, and only 17% at the L_{HK} of 30 μm. Although the FOM takes the total gate charges into consideration instead of the gate-to-drain charges only, HKTMOS still exhibits a significant FOM improvement over that of SJ.

Charge imbalance between N&P drift region in actual fabrication process is another issue of the SJ, even slight charge imbalance caused by doping difference can severely impact the BV of SJ device. Adversely, HKTMOS exhibit excellent doping difference tolerance because their BVs not only depend on charge balance but also PM effect from HK trench. As Figure 4 shows, with the rise of the N&P drift region doping difference, the BV of HKTMOS with ε_{HK} =400 almost remains unchanged. However, smaller ε_{HK} value always causes higher BV sensitivity to doping difference, this is because with smaller ε_{HK}, the PM capability of HK trench is impaired, consequently, the BV drops more rapidly with the rise of doping difference. As the BV of SJ solo relies on the charge balance and free of PM effect, SJ gives the worst performance. The BV of SJ at the doping difference of 4 ± 10^{-16}cm^{-3} drops to 30% of the BV under the charge-balance condition.

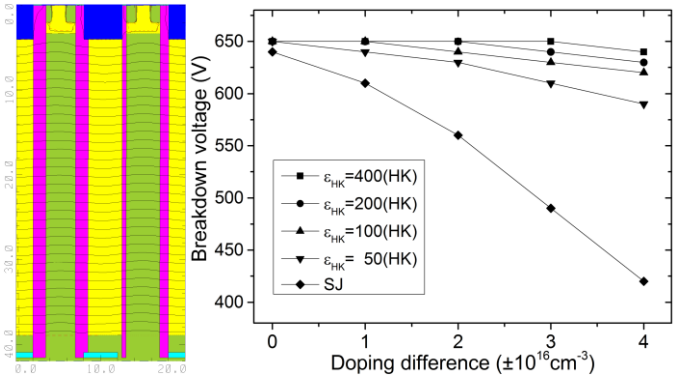

Fig 4. (a) The potential distribution for a HKTMOS with L_{HK} of 39 μm and HK trench randomly shifted in both width and position. (b) The impact of charge-imbalance to BV for SJ and HKTMOS with different ε_{HK} for the device length of 39 μm under the baseline doping of 10^{15} cm^{-3} for both N and P pillar.

4 Conclusion

The HKTMOS we proposed in this letter indicates excellent performance for wide BV range according to investigation. Its FOM is predictable using the HKTMOS constant and shows significant improvement than that of the SJ. Besides, HKTMOS also demonstrates its good charge-imbalance tolerance than its SJ counterparts. Above all, the HKTMOS is potential for the application on the energy conversion system for better efficiency and further promotion of the silicon limit.

References

1. X. Chen, “Super-junction voltage sustaining layers with alternating semiconductor and high-K dielectric regions,” U.S. Patent, 7230310B2, Jun. 12, 2007
2. X. Luo, Y. Jiang, K. Zhou, P. Wang, X. Wang, Q. Wang, G. Yao, B. Zhang, and Z. Li, “Ultralow specific on-resistance superjunction vertical DMOS with high-K dielectric pillar,” IEEE Electron Device Lett., vol. 33, no. 7, pp. 1042–1044, Jul. 2012.
3. J. Li P. Li, W. Huo, G. Zhang, Y. Zhai, and X. Chen, “Analysis and fabrication of an LDMOS with high-permittivity dielectric,” IEEE Electron Device Lett., vol. 32, no. 9, pp. 1266–1268, Sep. 2011.
4. X. Chen and J. Sin. “Optimization of the specific on-resistance of the COOLMOS (TM),” IEEE Trans. Electron Devices, vol. 48, no. 2, pp. 344-348, Feb. 2001.
5. B. J. Baliga, T. Syau, and P. Venkatraman, “The accumulation-mode field effect transistor: a new ultralow on-resistance MOSFET” IEEE Electron Device Lett., vol. 13, no. 8, pp. 427–429, Aug. 1992.
6. B. J. Baliga, "Fundamentals of power semiconductor devices," Springer-Verlag, 2008, pp. 362.
7. B. J. Baliga, "Advanced power MOSFET concepts," Springer-Verlag, 2010, pp. 55.